THE COLLEGE OF AERONAUTICS
CRANFIELD

CRACK FORMATION IN BLANKING AND PIERCING

by

C.F. Noble and P.L.B. Oxley

NOTE NO. 139

February, 1963

THE COLLEGE OF AERONAUTICS

CRANFIELD

CRACK FORMATION IN BLANKING AND PIERCING

- by -

C.F. Noble, D.C.Ae., and P.L.B. Oxley, B.Sc., Ph.D.*

SUMMARY

In recent experiments on blanking and piercing, it was found that cracks occurred in the region of maximum hardness gradient and that cracking could be eliminated by radiusing the punch and die edges. In this paper, a simple stress analysis is made of the corresponding plane strain deformation, account being taken of the strain-hardening property of the work material. The above experimental observations are then shown to be compatible with the predicted stress distributions.

---

* Respectively, Research Engineer and Senior Lecturer, Department of Production and Industrial Administration, The College of Aeronautics, Cranfield.

CONTENTS

1. INTRODUCTION

In blanking and piercing, a hole is punched in a sheet, the removed metal being constrained to pass through a die (Fig. 1.). The difference in the processes is that, in blanking, it is the outside contour that is formed, i.e. X (Fig. 1.) is the required component, while in piercing, a hole is formed in the required component, i.e. Y (Fig. 1.). The deformation in these processes is essentially a simple shearing along the line AB (Fig. 1.) which joins the punch and die edges. If cracking in the deformed metal can be eliminated or confined to the waste material, then the formed edge of the component is greatly improved and additional finishing operations are not required.

2. EXPERIMENTAL RESULTS

Recent experiments (Ref. 1) have shown that cracking can be eliminated, e.g. by radiusing the punch and die edges. In these experiments, partly pierced and partly blanked specimens were produced and sectioned as shown in Fig. 2. The edges of the punches and dies were varied in shape to enable the effect of tool geometry to be assessed. Specimens, when polished and etched and examined microscopically, revealed a severely deformed zone (Fig. 3) which was approximately symmetrical about AB (Fig. 1). A micro-hardness survey of this zone was made and, in this way, contours of constant hardness were traced out. Figs. 4 to 7 show examples of these surveys. In all cases the work material was annealed 0.1% carbon steel.

The main finding of the investigation was that when cracks occurred, they were confined to the regions of maximum hardness gradient, i.e. regions in which the rate of change of hardness was a maximum. Figs. 4 and 6 show examples of cracks and it can clearly be seen that cracks have occurred where the hardness contours are grouped most closely together. Fig. 7 shows that by radiusing the edges of the punch and die, the hardness gradient is decreased and cracking is eliminated. Figs. 5 and 6 show that, by radiusing either the die edge (blanking) or the punch edge (piercing), cracking can be confined to the waste material. Tests on hard copper and soft copper showed that the hardness gradient was greater for the soft copper and that cracking was more likely to occur for this condition of the material. Figs. 8 and 9 show photomicrographs for hard and soft copper.

In the work described, no explanation, in terms of the mechanics of the process, was advanced to explain the coincidence of cracks with the zone of maximum hardness gradient.

3. ANALYSIS AND DISCUSSION OF EXPERIMENTAL RESULTS

In this paper, a stress analysis of the deformation in the actual blanking process is not attempted. Instead, the problem is simplified by considering the corresponding plane strain deformation, shearing, in which the deformation is essentially the same as for blanking. It is then shown that such experimental observations, as the crack occurring in the region of maximum hardness gradient and hard copper showing less tendency to crack than soft copper, are compatible with the calculated stresses.

Consider the shearing process represented by Fig. 10, where $w \gg t$, i.e. plane strain condition. From theoretical considerations we might expect that the deformation would simply be a shearing along the line joining A and B. While this is a possible mode of deformation for the ideal non-strain-hardening material, it follows from equilibrium considerations that if the material strain-hardens, then the line AB must broaden into a finite shear zone. From symmetry, the material within the shear zone can be expected to have a maximum hardness and hence shear flow stress, along AB (where the shear strain will be a maximum), the hardness and shear flow stress decreasing to their values in the undeformed material on either side of AB. The general form of hardness and shear flow stress distribution is shown diagrammatically in Fig. 11.

Let us assume that the shear zone can be represented as shown in Fig. 12(a) where CD, AB and EF are parallel and represent directions of maximum shear stress. Consider the equilibrium of the small element of the shear zone shown in Fig. 12(b), the sides of the element being parallel to the directions of maximum shear stress. The normal stress on the sides of the element is the hydrostatic stress. Resolving forces parallel to AB, we obtain the equation

$$\Delta p = \frac{-\Delta k}{\Delta x} \Delta y \qquad \text{.... (1)}$$

where p is the hydrostatic stress (taken +ve when compressive), k is the shear flow stress (taken +ve when it exerts an anticlockwise moment on the element on which it acts) and x and y are measured as shown in Fig. 12. According to Equation (1), the variation of p along a line of maximum shear stress depends on the rate of change of shear flow stress normal to the considered line, i.e., $\frac{\Delta k}{\Delta x}$.

Applying Equation (1) along CD, one obtains

$$p_D = p_c - \sum_{0}^{\ell} \frac{\Delta k}{\Delta x} \Delta y \qquad \text{.... (2)}$$

where p_c and p_D are the hydrostatic stresses at C and D respectively and ℓ (Fig. 12) is the length of the shear zone. As $\frac{\Delta k}{\Delta x}$ is positive on the left hand side of AB (Fig. 11), this equation predicts that p_D will have a lower compressive value than p_c. If $\frac{\Delta k}{\Delta x}$ is large, then p_D can conceivably be tensile. Therefore, as cracking can be expected in regions of tensile p, this equation predicts that if cracking occurs, it will occur in the region of D. This is in agreement with experiment, e.g. Fig. 4. The tensile hydrostatic stress can be expected to be a maximum in the zone where $\frac{\Delta k}{\Delta x}$ is a maximum (i.e. from Equation (2)) and, because of the relationship between hardness and shear flow stress, this zone will also be the zone of maximum hardness gradient. We expect, from this argument, that cracking will occur in the region of maximum hardness gradient and this has been clearly demonstrated by the experimental work (Figs. 4 and 6).

For the line EF

$$p_F = p_E - \sum_{0}^{\ell} \frac{\Delta k}{\Delta x} \Delta y \qquad \text{.... (3)}$$

where p_E and p_F are the hydrostatic stresses at E and F. To the right of AB, $\frac{\Delta k}{\Delta x}$ is negative (Fig. 11) and, therefore, according to this equation, p_E will be less compressive than p_F.* If the stresses p_c and p_F are equal and $\frac{\Delta k}{\Delta x}$ has the same magnitude along CD and EF, then p_D and p_E will be equal and cracking can be expected to occur at E as well as at D. Fig. 4 shows an example of this. In practice, the sheet, in blanking and piercing, will bend under the action of the punch force in such a way that p_F can be expected to be greater than p_c; p_D will then be smaller than p_E and cracking will be more likely to occur at D than at E.

When the edges of the punch and die are radiused (Fig. 7), the width of the shear zone increases and the value of $\frac{\Delta k}{\Delta x}$ is reduced. It follows, from Equations (2) and (3), that the hydrostatic stresses at D and E are increased and, therefore, that cracking is reduced or eliminated. In blanking, only the die need be radiused (Fig. 5). The value of $\frac{\Delta k}{\Delta x}$, in

---

* By considering equilibrium in the 'x' direction (Fig. 12) as well as the 'y' direction, it can be shown that the lines of maximum shear stress are not straight, as assumed, but curved. However, a more detailed analysis of the shear zone, using variable flow stress slip-line theory, shows that the stress distribution found in this paper is essentially correct. The arguments presented to explain cracking are, therefore, unaffected.

the region of D, is thus reduced and cracking in this region can be eliminated. The value of $\frac{\Delta k}{\Delta x}$ is not reduced in the region of E and cracking occurs in the waste material (Fig. 5). A similar argument can be applied to piercing, in which case only the punch edge need be radiused (Fig. 6).

The relationship between the value of $\frac{\Delta k}{\Delta x}$ and the slope of the corresponding plastic stress-strain curve of the work material does not appear to be as simple as at first might be expected. That is, although, for a given set of conditions, we might expect that an increase in slope will given an increase in $\frac{\Delta k}{\Delta x}$ (Δk = shear strain $\times$ slope), it is not at all certain that there is a one to one relationship. Recent cutting experiments (Ref. 2) (the shear zone in cutting is similar to the shear zone in blanking and piercing) have shown that when the slope increases, the width of the shear zone (Δx) also increases (Fig. 13) and that, as a result of this, $\frac{\Delta k}{\Delta x}$ does not increase by a corresponding amount. It can be argued that, in cutting, the width of the shear zone (Δx) is determined far more by the work material properties than by tool geometry, whereas in blanking and piercing, this width is largely determined by the size of the radius on the punch and die edges. If this is the case, then we would expect that, in blanking and piercing, a much closer relationship would exist between $\frac{\Delta k}{\Delta x}$ and the slope of the corresponding plastic stress-strain curve. Further experiments will have to be made to investigate this point. At this stage we can only conclude that an increase in slope gives rise to some increase in $\frac{\Delta k}{\Delta x}$ and, therefore, that the more rapid a material's rate of strain-hardening, the more likely it is to crack. The results for soft copper and hard copper (Figs. 8 and 9) support this. An increase in rate of strain, resulting from an increase in punch speed, will give a lower slope of plastic stress-strain curve (Fig. 14 shows stress-strain curves for different rates of strain obtained from cutting tests (Ref. 3). Therefore, following the above argument, an increase in punch speed will give a lower value of $\frac{\Delta k}{\Delta x}$ and cracking will be reduced. Experiments appear to confirm this (Ref. 4).

It has not been attempted in this paper to determine the actual magnitudes of stress and strain at which cracks occur. Further work is clearly needed to establish a suitable crack criterion before the above analysis can be used predictively in the design of punches and dies.

ACKNOWLEDGEMENTS

The authors wish to thank the Production Engineering Research Association of Great Britain (P.E.R.A.) for permission to quote so freely from their report Number 93.

References

1. P.E.R.A. Report No. 93, 1961.

2. Oxley, P.L.B., Humphreys, A.G., and Larizadeh, A. "The influence of rate of strain-hardening in machining". Proc. Inst. Mech. Engrs. Vol. 175, 1961, pp. 881 - 917.

3. Oxley, P.L.B. "Rate of strain effect in metal cutting" Trans. A.S.M.E., Paper No. 62-WA-139, 1963.

4. Willis, J. "Deep drawing" Butterworths Scientific Publications. 1954. p. 102.

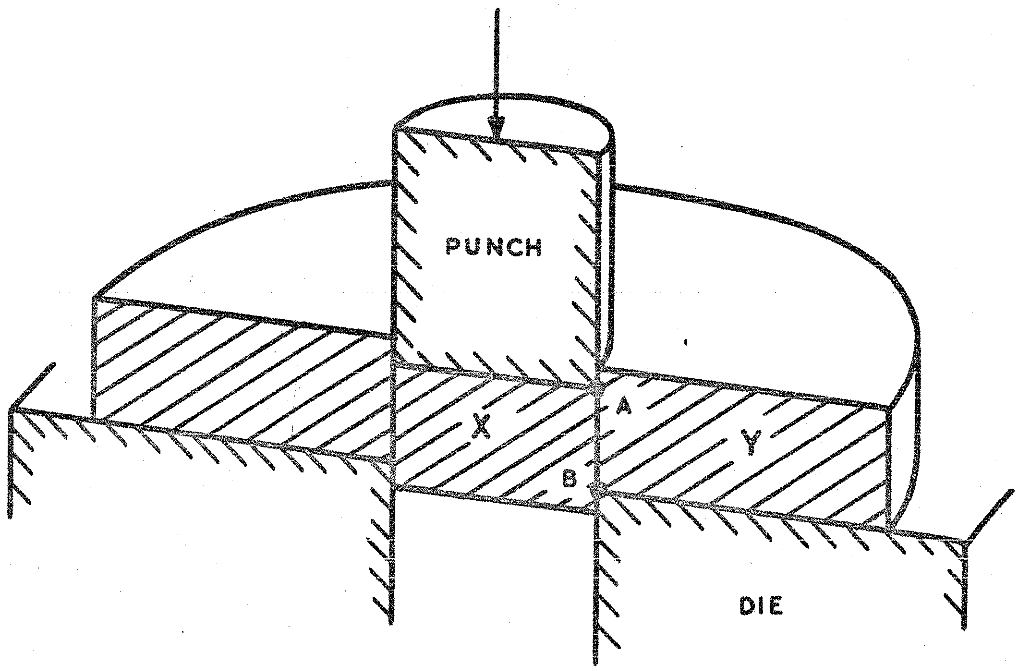

FIG. 1. SECTION THROUGH PUNCH AND DIE.

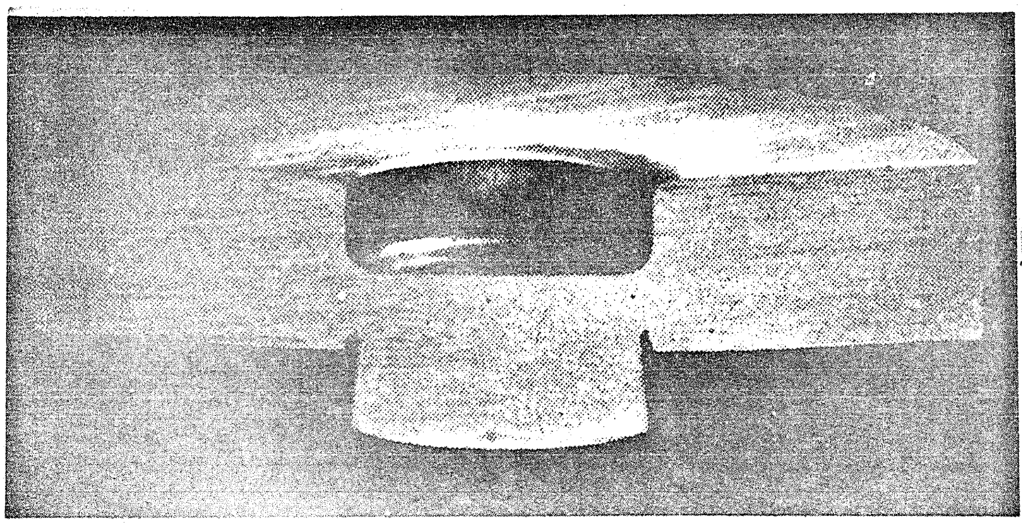

APPROX X 2

FIG. 2. SECTION OF PARTLY PIERCED SPECIMEN.

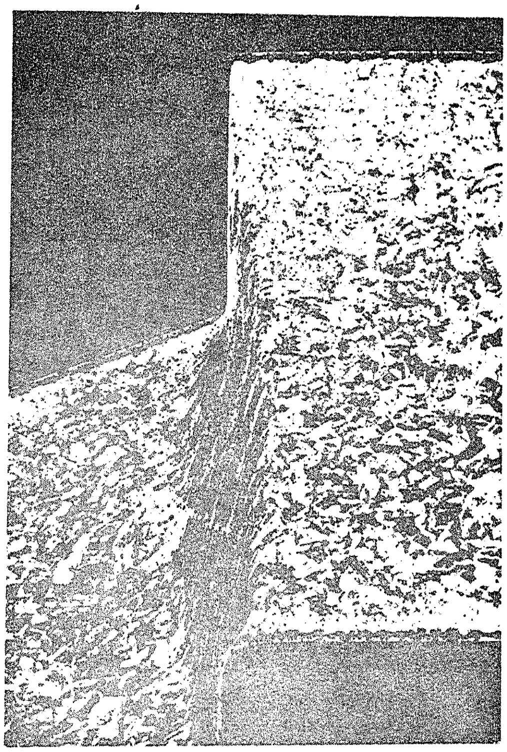

X 25

FIG. 3. PHOTOMICROGRAPH OF SEVERELY DEFORMED ZONE.

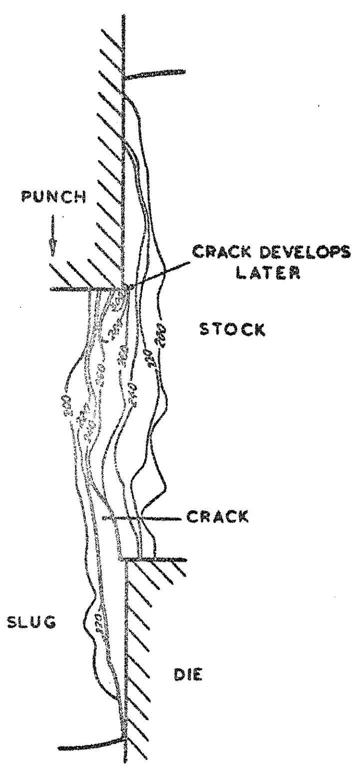

FIG. 4. HARDNESS SURVEY.

SQUARE EDGE PUNCH
— SQUARE EDGE DIE.

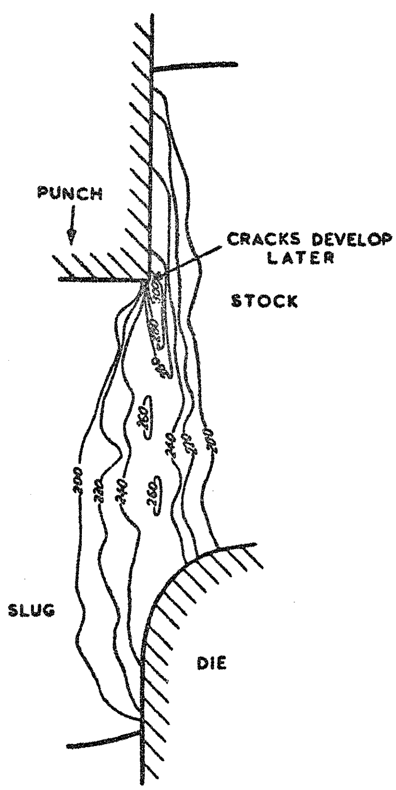

FIG. 5. HARDNESS SURVEY.

SQUARE EDGE PUNCH
— RADIUS EDGE DIE.

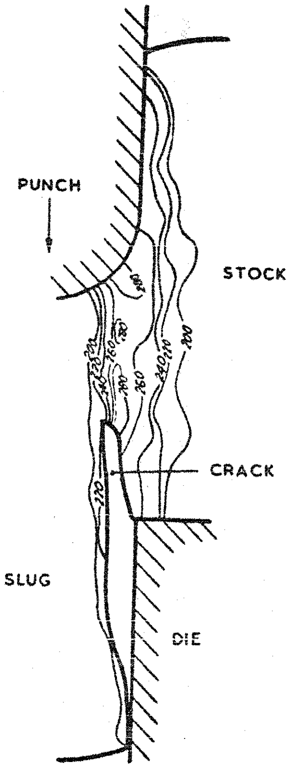

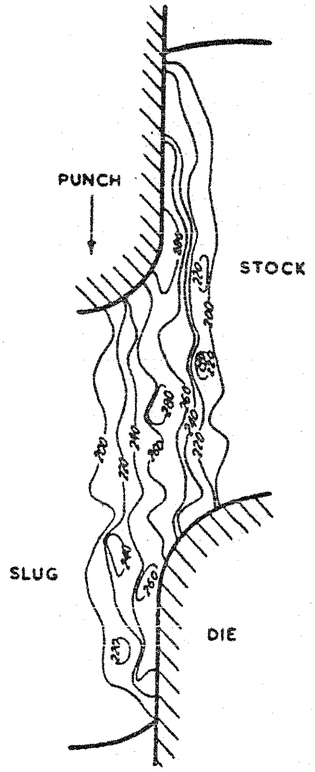

FIG. 6. HARDNESS SURVEY.
RADIUS EDGE PUNCH
— SQUARE EDGE DIE.

FIG. 7. HARDNESS SURVEY.
RADIUS EDGE PUNCH
— RADIUS EDGE DIE.

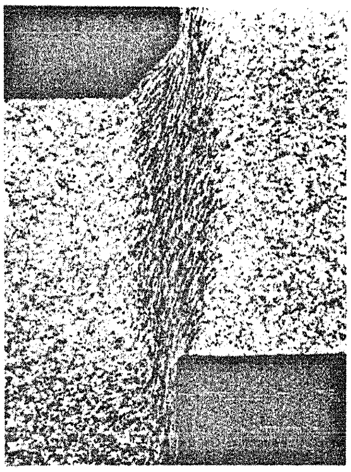

X 7·5

FIG. 8. PHOTOMICROGRAPH OF DEFORMED ZONE FOR HARD COPPER.

FIG. 9. PHOTOMICROGRAPH OF DEFORMED ZONE FOR SOFT COPPER.

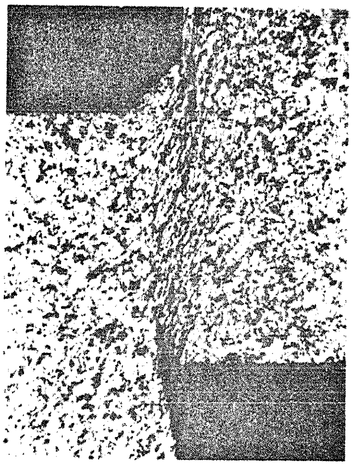

X 7·5

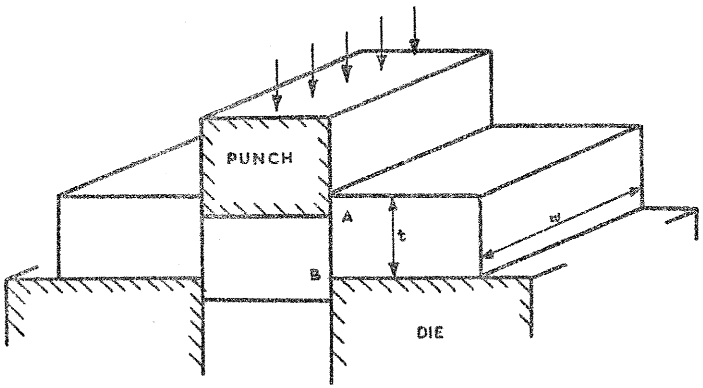

FIG. 10. PLANE-STRAIN SHEARING $\omega >> t$

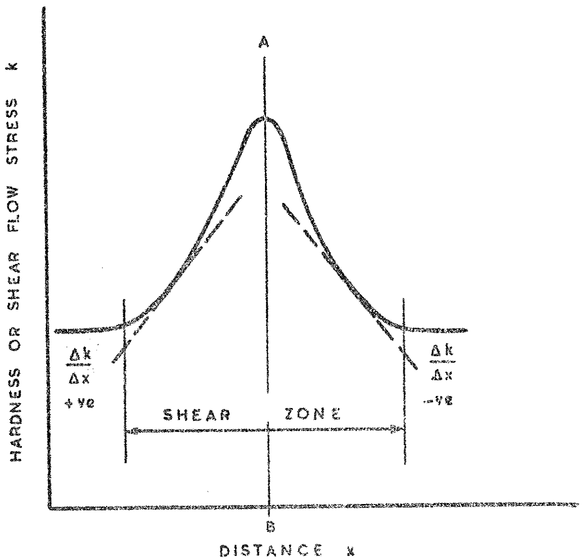

FIG. 11. HARDNESS AND SHEAR FLOW STRESS DISTRIBUTION.

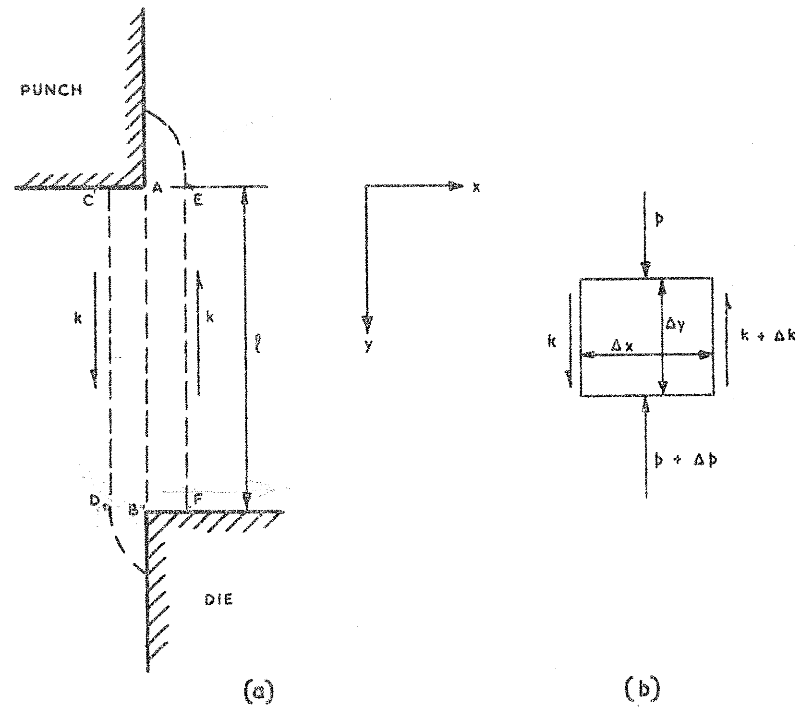

FIG. 12. IDEALIZED SHEAR ZONE AND ELEMENT OF SHEAR ZONE.

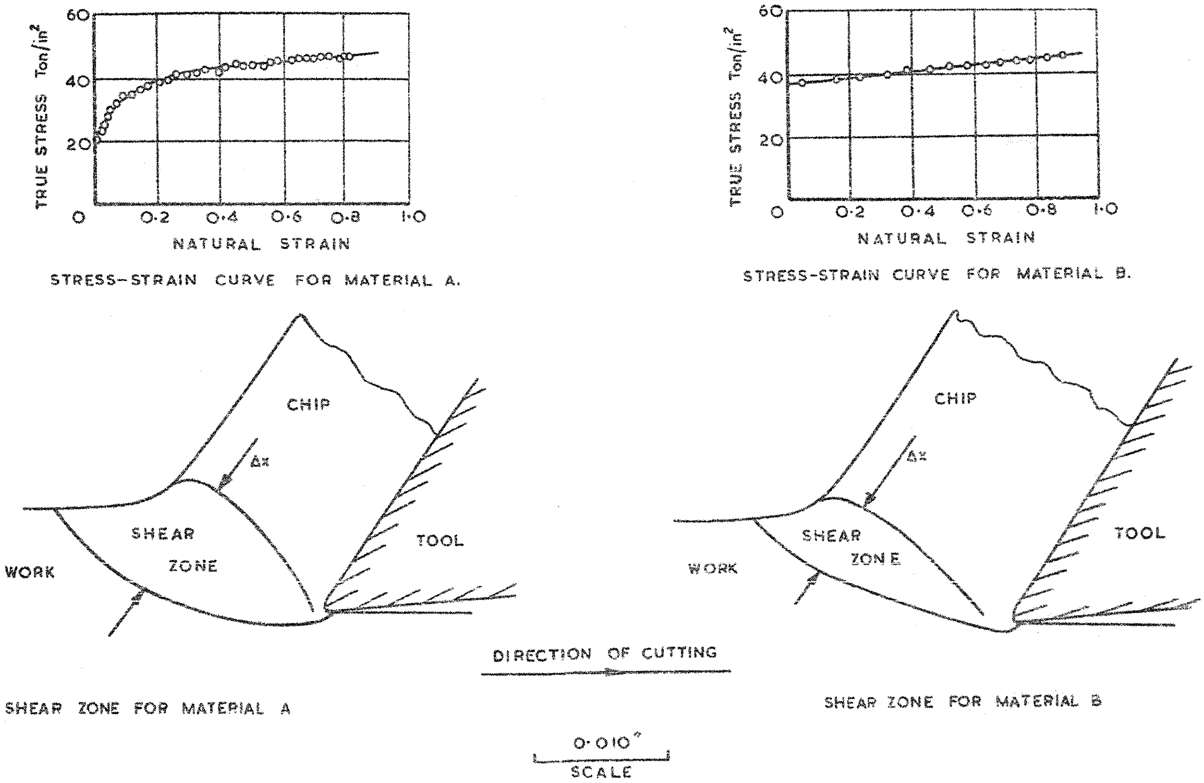

FIG. 13. SHEAR ZONES IN CUTTING

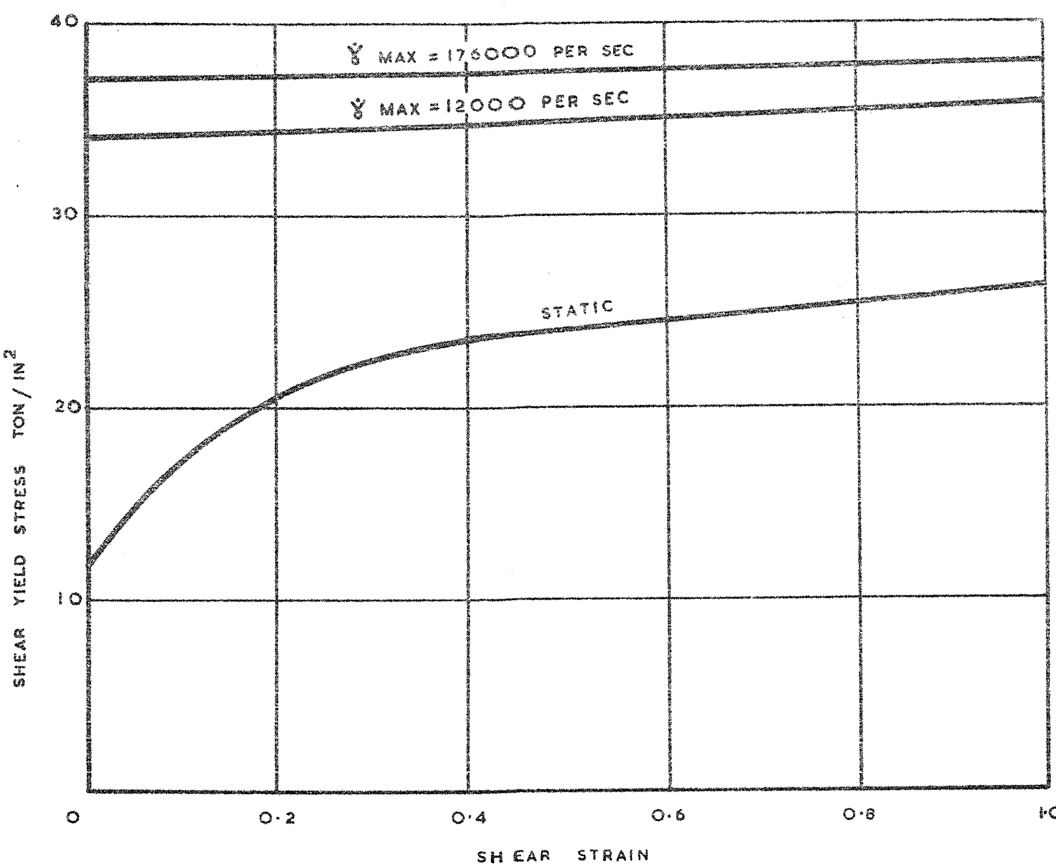

FIG. 14. STRESS – STRAIN CURVES FOR DIFFERENT STRAIN RATES.